

Preparation and evaluation of SiO_2 -deposited stearic acid-g-chitosan nanoparticles for doxorubicin delivery

Hong Yuan
Xin Bao
Yong-Zhong Du
Jian You
Fu-Qiang Hu

College of Pharmaceutical Sciences,
Zhejiang University, Hangzhou, PR
China

Purpose: Both polymer micelles and mesoporous silica nanoparticles have been widely researched as vectors for small molecular insoluble drugs. To combine the advantages of copolymers and silica, studies on the preparation of copolymer-silica composites and cellular evaluation were carried out.

Methods: First, a stearic acid-g-chitosan (CS-SA) copolymer was synthesized through a coupling reaction, and then silicone oxide (SiO_2)-deposited doxorubicin (DOX)-loaded stearic acid-g-chitosan (CS-SA/ SiO_2 /DOX) nanoparticles were prepared through the sol-gel reaction. Physical and chemical properties such as particle size, zeta potential, and morphologies were examined, and small-angle X-ray scattering (SAXS) analysis was employed to identify the mesoporous structures of the generated nanoparticles. Cellular uptake and cytotoxicity studies were also conducted.

Results: CS-SA/ SiO_2 /DOX nanoparticles with different amounts of SiO_2 deposited were obtained, and SAXS studies showed that mesoporous structures existed in the CS-SA/ SiO_2 /DOX nanoparticles. The mesoporous size of middle-ratio and high-ratio deposited CS-SA/ SiO_2 /DOX nanoparticles were 4–5 nm and 8–10 nm, respectively. Based on transmission electron microscopy images of CS-SA/ SiO_2 /DOX nanoparticles, dark rings around the nanoparticles could be observed in contrast with CS-SA/DOX micelles. Furthermore, CS-SA/ SiO_2 /DOX nanoparticles exhibited faster release behavior in vitro than CS-SA/DOX micelles; cellular uptake research in A549 indicated that the CS-SA/ SiO_2 /DOX nanoparticles were taken up by A549 cells more rapidly, and that CS-SA/ SiO_2 /DOX nanoparticles entered the cell more easily when the amount of SiO_2 was higher. IC_{50} values of CS-SA/DOX micelles, CS-SA/ SiO_2 /DOX-4, CS-SA/ SiO_2 /DOX-8, and CS-SA/ SiO_2 /DOX-16 nanoparticles against A549 cells measured using the MTT assay were 1.69, 0.93, 0.32, and 0.12 $\mu\text{g}/\text{mL}$, respectively.

Conclusion: SiO_2 -deposited stearic acid-g-chitosan organic-inorganic composites show promise as nanocarriers for hydrophobic drugs such as DOX.

Keywords: doxorubicin, nanoparticles, SiO_2 -deposited, stearic acid-g-chitosan

Introduction

Currently, the nano drug delivery system (NDDS) is widely studied in the field of pharmaceutical science.¹ An NDDS can be delivered to a specific site *in vivo* to release drugs, and is a combination of drugs and nano-sized carriers (such as polymeric micelles, solid lipid nanoparticles, nanospheres, and liposomes). NDDS presents several advantages such as reducing side effects, prolonging circulation time, and a passive targeting effect compared with traditional drug preparations.

Polymeric micelles are some of the most common nanocarriers; they can be formed through self-assembly of amphiphilic copolymers.² In an aqueous environment,

Correspondence: Hong Yuan;
Fu-Qiang Hu
College of Pharmaceutical Sciences,
Zhejiang University, 866 Yuhangtang
Road, Hangzhou 310058, PR China
Tel/fax +86 571 8820 8439
Email yuanhong70@zju.edu.cn;
hufq@zju.edu.cn

hydrophobic chains of the amphiphilic copolymer can aggregate into the inner core through hydrophobic interactions while the hydrophilic chains form the outer shell of micelle. The hydrophobic core serves as a reservoir for hydrophobic drugs, leading to improved bioavailability of insoluble drugs by increasing their solubility. The size of polymeric micelles is generally on the nanoscale (10–100 nm) and can spontaneously accumulate in tumor tissues through their well-known “enhanced permeability and retention (EPR) effect,”¹³ marking it as a candidate carrier for antitumor drugs. In addition, the surface charge of polymeric micelles makes them suitable as carriers for biomacromolecules such as genes,^{4–6} vaccines,⁷ and protein drugs,⁸ protecting these biomacromolecules from degradation via oral drug delivery systems.

In addition to being carriers of organic materials, inorganic carriers such as mesoporous silica nanoparticles (MSNs) are widely studied. MSNs, which are amorphous silicon oxide materials, possess a highly ordered pore structure⁹ and have a single pore size distribution ranging from 2–50 nm. The ordered pore structure of MSNs possesses very large surface area and specific pore volume; therefore, drugs can be stored in this space.¹⁰ The drug release rate can be controlled by regulating the size of mesopores. Slowing et al¹¹ and Radu et al¹² showed that the mesoporous silicon was biocompatible and a relatively safe carrier material based on toxicity studies against animal cells.

Both organic and inorganic carriers have their respective advantages. Recently, many studies have focused on the composite materials of organic polymers and mesoporous silicon materials. Previous studies have revealed that organic–inorganic composite materials exhibit more favorable characteristics when applied in drug delivery systems, such as thorough drug release behavior,¹³ more efficient solubilization for insoluble drugs,¹⁴ higher bioavailability,^{13,14} and more prominent biological stability.^{15,16} Therefore, studies examining composites of organic nanoparticles and mesoporous silica have considerable application value.

Chitosan is an organic polymer material with properties such as low toxicity and biodegradation. Synthesized by coupling reaction between the amino groups of chitosan and the carboxyl groups of stearic acid, stearic acid-g-chitosan (CS-SA) can self-assemble into micelles in an aqueous environment and presents excellent solubilization and drug-encapsulating capabilities.¹⁷ The goal of this study was to evaluate the feasibility of composite of CS-SA and mesoporous silica as a drug carrier and to contrast the advantages and disadvantages of this composite when applied as an NDDS.

The sol-gel reaction¹⁸ (two steps, including hydrolysis and polycondensation) was employed to prepare silicon dioxide-deposited stearic acid-g-chitosan (CS-SA/SiO₂) composite nanoparticles. Using doxorubicin (DOX) as a model drug, the effects of silica crosslinking on drug-loading capacity, drug release in vitro, cellular uptake, and cytotoxicity against human lung adenocarcinoma A549 cells were investigated in detail.

Materials and methods

Materials

Chitosan of low molecular weight ($M_w = 18.0$ kDa) was prepared by enzymatic degradation¹⁹ of chitosan ($M_w = 450$ kDa, 95% deacetylated degree), which was purchased from Yuhuan Marine Biochemistry Co, Ltd (Zhejiang, China). Stearic acid was purchased from Wenzhou Huaqiao Chemical Reagent Co, Ltd (Wenzhou, China). Chitosanase was obtained from Dyadic International, Inc (Jupiter, FL). 1-Ethyl-3-(3-dimethylaminopropyl) carbodiimide hydrochloride (EDC · HCl) was purchased from Shanghai Medpep Co, Ltd (Shanghai, China). 2,4,6-trinitrobenzene sulfuric acid, 3-(4, 5-dimethylthiazol-2-yl)-2,5-diphenyltetrazolium bromide (MTT), and pyrene were purchased from Sigma-Aldrich (St Louis, MO). Acetone, acetic acid, and ethanol were supplied from Hangzhou Chemical Reagent Co, Ltd. Tungstophosphoric acid and hexadecyltrimethylammonium bromide (CTAB) were purchased from Aladdin Reagent Co, Ltd (Shanghai, China). Doxorubicin hydrochloride (DOX · HCl) was obtained from Zhejiang Hisun Pharm Co, Ltd (Zhejiang, China). Tetraethoxy-silicone (TEOS) and isopropanol were purchased from Shuanglin Chemical Reagent Co, Ltd (Hangzhou, China). RPMI 1640 medium and fetal bovine serum were purchased from Gibco BRL (Life Technologies, Carlsbad, CA). All other chemicals were of analytical or chromatographic grade.

Synthesis and characterization of CS-SA conjugate

The CS-SA conjugate was synthesized via a coupling reaction of the carboxyl groups of stearic acid (SA) with the amino groups of chitosan (CS; $M_w = 18.0$ kDa) in the presence of EDC · HCl.^{20,21} Briefly, 3 g CS was dissolved in 100 mL distilled water and heated to 60°C. Next, 1.5 g SA (30% of the molar amount of amino groups in CS) and 5.25 g EDC · HCl (EDC · HCl: SA = 5:1, mol:mol) were dissolved in a solution of 35 mL acetone and 15 mL ethanol. After stirring for 30 minutes at 400 rpm (maintained at 60°C), the solution was added to the CS aqueous solution and stirred

for another 8 hours. Next, the reaction solution was dialyzed against acetic acid water solution (pH 3.0) using dialysis membrane (MWCO: 7 kDa; Spectrum Laboratories, Laguna Hills, CA) for 24 hours. The dialysate was changed to deionized (DI) water, dialyzed for another 24 hours, and the reaction solution lyophilized. The lyophilized product was further purified with ethanol to remove the byproduct. Finally, the product CS-SA was redispersed in DI water and lyophilized again.

The structure of received CS-SA was confirmed using ¹H-nuclear magnetic resonance (NMR) analysis using an NMR spectrometer (AC-80; Bruker BioSpin, Rheinstetten, Germany). CS and CS-SA were dissolved in D₂O solution, and SA was dissolved in diethyl sulfoxide (DMSO)-d₆. The concentration was 10 mg/mL.

The critical micelle concentration (CMC) of the synthesized CS-SA was determined by fluorescence spectroscopy using pyrene as a probe.²² A fluorometer (F-2500; HITACHI Co, Tokyo, Japan) was used to record fluorescence spectra. The excitation wavelength was 337 nm, and the slits were set at 2.5 nm (excitation) and 10 nm (emission). The intensities of the emission were monitored at a wavelength range of 337–450 nm. The intensity ratios (I₁/I₃) of the first peak (I₁, 374 nm) to the third peak (I₃, 385 nm) were plotted versus the sample concentration to determine CMC.

Preparation of DOX-loaded CS-SA micelles

DOX was obtained by the reaction²³ of DOX · HCl and triethylamine in DMSO overnight. Following dialysis and lyophilization, 1 mg/mL DOX/DMSO solution was prepared. Next, 100 mg CS-SA was dissolved in 100 mL DI water, and then 5 mL DOX/DMSO solution (1 mg/mL) was added. After dialysis against DI water using a dialysis membrane (MWCO: 7 kDa; Spectrum Laboratories) for 24 hours, the product was centrifuged at 4000 rpm for 10 minutes to remove precipitated drug, and the final product of DOX-loaded CS-SA micelles (CS-SA/DOX) was obtained.

Preparation of SiO₂-deposited DOX-loaded nanoparticles

SiO₂-deposited DOX-loaded CS-SA (CS-SA/SiO₂/DOX) nanoparticles were prepared by mixing silica precursor (TEOS) and DOX in an appropriate solvent, which was added into the CS-SA solution. Nanoparticles with different SiO₂-deposited ratios were prepared by adding different amount of TEOS. Briefly, 1 mg/mL CS-SA/H₂O solution, 1 mg/mL DOX/DMSO solution, and 10 mg/mL CTAB/isopropyl alcohol solution were prepared. Next, 400 μL

(800 μL, 1600 μL) of TEOS was added into 5 mL of DOX/DMSO solution (1 mg/mL) and vortexed for 1 min. The mixed solution was added into 100 mL CS-SA/H₂O solution and stirred at room temperature. After 10 min of stirring, the pH of the mixed solution was adjusted to 3.0 and stirred for another 10 min. Subsequently, 5 mL CTAB/isopropyl alcohol solution (10 mg/mL) was added into the reaction system in a dropwise manner and allowed to react for 4 hours. The pH of the reaction mixture was adjusted to 7.0, and the reaction was allowed to continue for another 4 h. CS-SA/SiO₂/DOX-4 (8, 16) nanoparticles were obtained using dialysis.

Characterization of CS-SA, CS-SA/DOX, micelles and CS-SA/SiO₂/DOX nanoparticles

Size and zeta potential

Micelle size and zeta potential of CS-SA micelles, CS-SA/DOX micelles, and CS-SA/SiO₂/DOX nanoparticles with a concentration of 1 mg/mL in DI water were determined by dynamic light scattering by using a Zetasizer analyzer (3000HS; Malvern Instruments Ltd, Malvern, UK).

Morphological observation

The examinations of internal structure and surface morphology for CS-SA micelles, CS-SA/DOX micelles, and CS-SA/SiO₂/DOX nanoparticles were performed using transmission electron microscopy (TEM) (JEM-1230; JEOL, Tokyo, Japan) and scanning electron microscopy (SEM) (SIRON, FEI; Hillsboro, OR), respectively.

Small-angle X-ray scattering (SAXS) analysis

Polycrystalline diffraction (D/MAX 2550/PC; RIGAKU, Tokyo, Japan) was used to investigate the periodic structure of CS-SA/SiO₂/DOX nanoparticles. SAXS patterns were recorded over the range of 2θ = 0.5°–5° using Cu Kα radiation.

Drug-loading capacity

Fluorescence spectrophotometry was used to determine the content of DOX in CS-SA/DOX micelles and CS-SA/SiO₂/DOX nanoparticles, with the excitation wavelength, emission wavelength, and slit at 505, 565, and 5 nm, respectively. A total of 10 μL DOX-loaded nanoparticles solution was diluted by adding a 100-fold volume of aqueous DMSO solution (DMSO:H₂O = 9:1, v/v). The DOX concentration (C₀, μg/mL) was measured and the drug encapsulation efficiency (EE; %) as well as drug loading amount (DL; %)

of DOX-loaded nanoparticles was calculated using the following equations:

$$\text{EE\%} = (C_0 \times V/M) \times 100\% \quad (1)$$

$$\text{DL\%} = [C_0 \times V/(W + C_0 \times V)] \times 100\%, \quad (2)$$

where C_0 is the drug concentration of the DOX-loaded nanoparticles solution, M is the weight of drug added in solution (μg), V was the total volume of DOX-loaded nanoparticle solution (mL), and W was the weight of copolymer CS-SA (μg).

In vitro release assay

The drug-release profiles of CS-SA/DOX micelles and CS-SA/SiO₂/DOX-4 (8, 16) nanoparticles were investigated using phosphate-buffered saline (PBS) solution (pH 7.4) as dissolution medium. CS-SA/DOX micelles and CS-SA/SiO₂/DOX-4 (8, 16) nanoparticle solution (containing 30 μg DOX) were withdrawn and diluted into 1 mL using DI water. After placing the sample in a dialysis bag (MWCO: 7 kDa; Spectrum Laboratories), the bag was placed into a plastic tube containing 30 mL of phosphate-buffered solution (PBS). The tube was then placed in a 37°C water bath and stirred at 60 rpm. At specific time intervals, the medium was exchanged with fresh medium. The DOX concentration of medium samples was detected using a fluorospectrophotometer with the consistent parameter settings described in a previous section. All drug-release tests were performed in triplicate.

Cell culture

A549 (the human lung adenocarcinoma cell line) cells were incubated in RPMI 1640 supplemented with 10% (v/v) fetal bovine serum and penicillin/streptomycin (100 U/mL, 100 U/mL) under a humidified atmosphere containing 5% CO₂ at 37°C.

Cellular uptake investigation

A549 cells were seeded at a density of 2.0×10^4 cells/well in a 24-well plate (Nalge Nunc International, Naperville, IL) and allowed to attach for 24 hours. Next, varying amounts of CS-SA/DOX micelles and CS-SA/SiO₂/DOX-4 (8, 16) nanoparticles were added (3 μg of DOX equivalent per well) for further incubation for 1, 2, 4, 8, 12, and 24 hours.

After washing with PBS three times, the cells were observed under a fluorescence microscope (DMIL; Leica Microsystems Ltd, Wetzlar, Germany).

Cytotoxicity assay

In vitro cytotoxicities of CS-SA/DOX micelles and CS-SA/SiO₂/DOX-4 (8, 16) nanoparticles against A549 cells were evaluated using the MTT assay. Cells were seeded at 5.0×10^4 cells/well in a 96-well plate (Nalge Nunc International). After a 24-hour incubation, CS-SA/DOX micelles and CS-SA/SiO₂/DOX-4 (8, 16) nanoparticles at various concentrations were added. The cells were further incubated for 24 hours. Next, 20 μL of MTT solution (5 mg/mL in DI water) was added to each well. After incubation for another 4 h, the culture medium was removed, and 200 μL DMSO was added to dissolve the formazan crystals. Finally, the plates were shaken for 10 minutes, and the absorbance of the formazan product was measured at 570 nm using a microplate reader (model 680; Bio-Rad, Hercules, CA). The percentage of cell inhibition was calculated based on the following equation:

$$\text{Cell inhibition \%} = (1 - A_{\text{treated}}/A_{\text{control}}) \times 100\%, \quad (3)$$

where A_{treated} and A_{control} represent the absorbance of treated wells and the control wells, respectively.

Statistical analysis

Data are expressed as the means of three separate experiments. Differences between groups were assessed using unpaired two-tailed Student's *t*-test and a *P*-value <0.05 was considered statistically significant in all cases.

Results and discussion

Synthesis and characteristics of CS-SA

CS-SA was synthesized by reacting the carboxyl group of SA and the amino groups of CS (18.0 kDa) in the presence of EDC · HCl. The structure of the obtained CS-SA conjugate was confirmed by the ¹H NMR spectrum (Figure 1). The proton peaks of CS and SA were observed on the ¹H NMR spectrum and were observed on the ¹H NMR spectrum of CS-SA. The results indicated that SA was successfully grafted onto the chains of CS.

The CMC of CS-SA in DI water was determined by fluorescence spectroscopy using pyrene as a probe. Figure 2A shows the ratios of the intensities (I_1/I_3) of the first peak (I_1 , 374 nm) to the third peak (I_3 , 385 nm) versus logarithm concentrations of CS-SA solution. The CMC of synthesized CS-SA, which indicates the intersection point, was 160 $\mu\text{g}/\text{mL}$. The relatively low CMC indicates that CS-SA could easily form into micelles through self-aggregation.

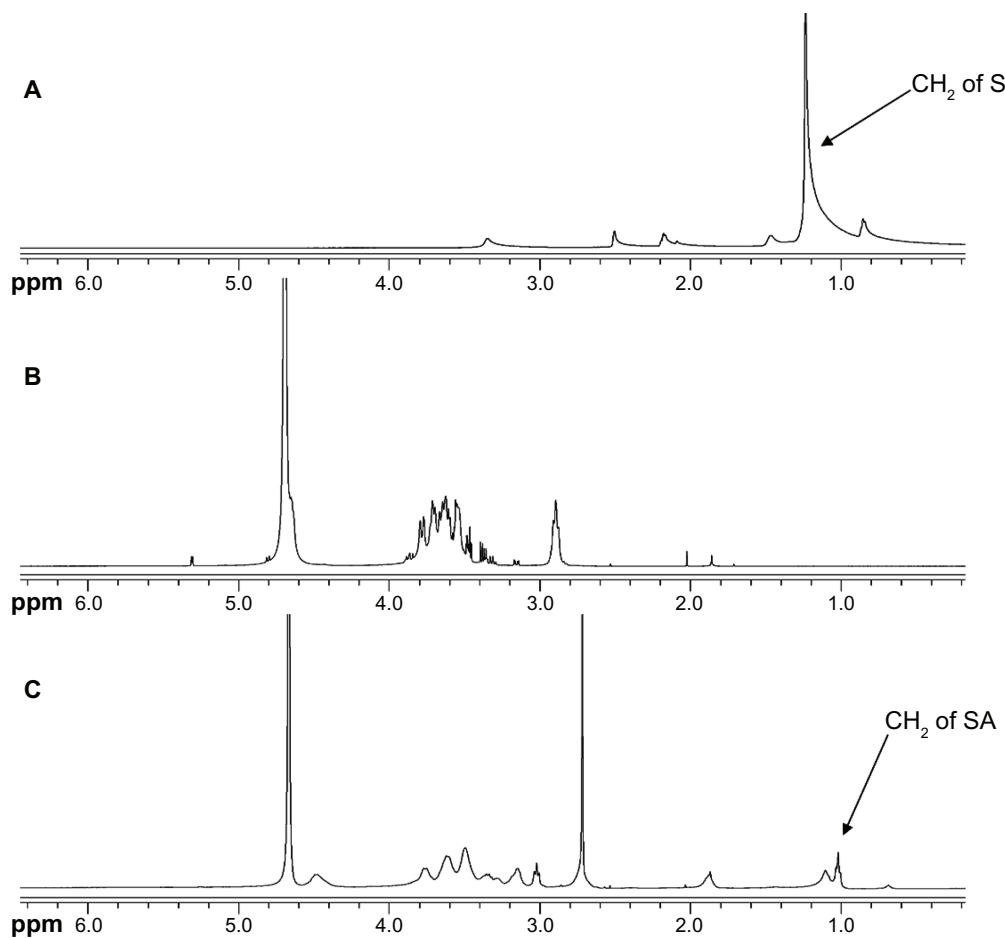


Figure 1 ¹H NMR spectrum for SA (A), CS (B), and CS-SA (C).

Abbreviations: CS, chitosan; SA, stearic acid.

As shown in Table 1, the average size and zeta potential of CS-SA micelles (1 mg/mL) were 117.5 ± 3.2 nm and 27.8 ± 2.9 mV, respectively. The average size determined by the Zetasizer coincided with that of the TEM image (Figure 2B).

Preparation and characteristics of CS-SA/DOX micelles and CS-SA/SiO₂/DOX nanoparticles

CS-SA/DOX micelles were prepared by the dialysis method. As shown in Table 1, the average size and zeta potential

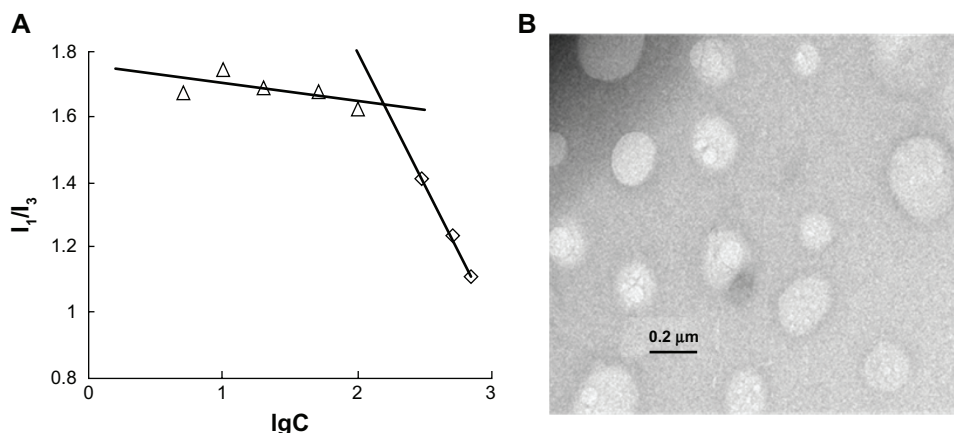


Figure 2 CMC determination of CS-SA micelles (A) and TEM image of CS-SA micelles (B).

Abbreviations: CMC, critical micelle concentration; CS, chitosan; SA, stearic acid; TEM, transmission electron microscopy.

Table 1 Properties of CS-SA micelles, CS-SA/DOX micelles, and CS-SA/SiO₂/DOX nanoparticles

Material	d _n (nm)	ξ (mV)	EE (%)	DL (%)
CS-SA	117.5 ± 3.2	27.8 ± 2.9	–	–
CS-SA/DOX	28.9 ± 0.5	45.0 ± 2.2	93.18	4.45
CS-SA/SiO ₂ /DOX-4	56.3 ± 0.6	15.6 ± 4.1	93.45	4.46
CS-SA/SiO ₂ /DOX-8	75.2 ± 1.1	19.0 ± 3.5	89.09	4.26
CS-SA/SiO ₂ /DOX-16	36.0 ± 0.3	17.8 ± 2.4	85.36	4.09

Note: Data represent the mean ± standard deviation (n = 3).

Abbreviations: d_n, number average diameter; ξ, zeta potential; CS, chitosan; DL, drug loading amount; DOX, doxorubicin; EE, encapsulation efficiency; SA, stearic acid.

of CS-SA/DOX were 28.9 ± 0.5 nm and 45.0 ± 2.2 mV, respectively. Compared with CS-SA micelles, there was a sharp decline in the particle size as well as some degree of increasing in zeta potential after DOX encapsulation. The size decrease may be due to hydrophobic interactions of DOX and the SA chain. When the feeding ratio of DOX to CS-SA was 1:20 (w/w), the EE% and DL% of CS-SA/DOX micelles were 93.2% and 4.45%, respectively.

CS-SA/SiO₂/DOX nanoparticles with different SiO₂-deposited ratios (CS-SA/SiO₂/DOX-4, CS-SA/SiO₂/DOX-8, and CS-SA/SiO₂/DOX-16) were prepared by adding different amount of TEOS. As presented in Table 1, the average size of CS-SA/SiO₂/DOX nanoparticles was between that of CS-SA micelles and CS-SA/DOX micelles, while the zeta potential was lower than that of CS-SA micelles. The generated crosslinked silica shell made the size of CS-SA/SiO₂/DOX larger than that of CS-SA/DOX. For the zeta potential, due to the silica shell around the surface of the particles, there were several silanols on the surface of CS-SA/SiO₂/DOX, leading to the decreased zeta potential. The EE% of CS-SA/SiO₂/DOX-4, CS-SA/SiO₂/DOX-8, and CS-SA/SiO₂/DOX-16 was 93.5%, 89.1%, and 85.4%, respectively, which demonstrated a slight decrease in the encapsulation efficiency with the increasing SiO₂-deposited ratio.

Figure 3A shows TEM images of CS-SA/DOX and CS-SA/SiO₂/DOX nanoparticles. In contrast with CS-SA/DOX, dark rings around the nanoparticles could be observed on all CS-SA/SiO₂/DOX nanoparticles images. This likely resulted from the SiO₂-deposition effect. During preparation, TEOS was introduced as a precursor for the Sol-Gel reaction, and the hydrolysis reaction was first carried out in acidic environment; the condensation reaction followed after the pH was adjusted to neutral. When the mixed solution was added (TEOS and DOX) into the CS-SA solution, DOX could enter into micelle cores using hydrophobic interaction, while TEOS dispersed in the water environment and took part in the Sol-Gel reaction. The reaction product, silanols, could

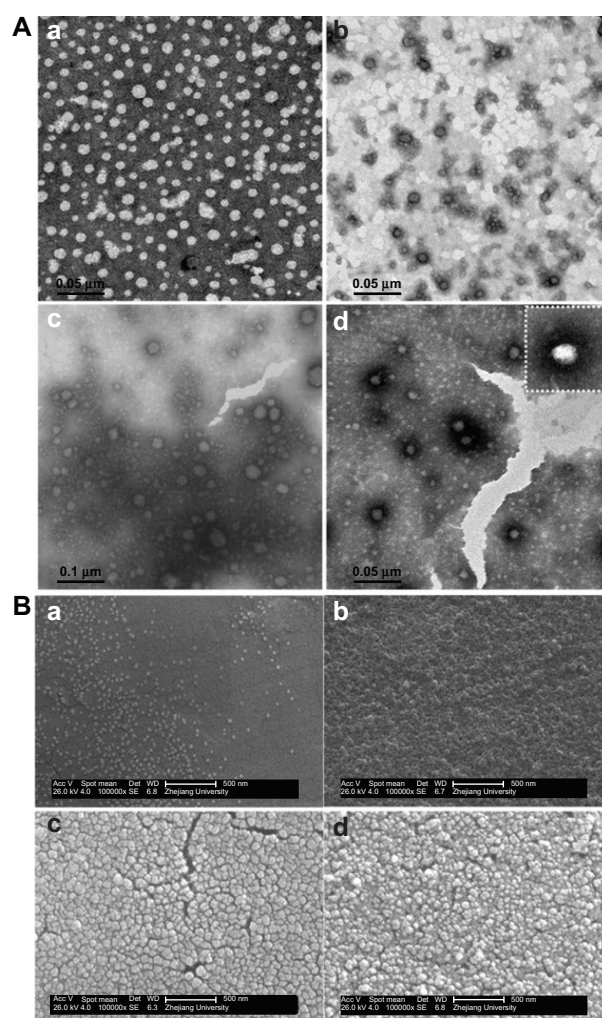


Figure 3 The TEM images (**A**) and SEM images (**B**) of CS-SA/DOX and CS-SA/SiO₂/DOX-4, 8, 16, where a-d represents CS-SA/DOX, CS-SA/SiO₂/DOX-4, CS-SA/SiO₂/DOX-8 and CS-SA/SiO₂/DOX-16 respectively.

Abbreviations: CS, chitosan; DOX, doxorubicin; SA, stearic acid; SEM, scanning electron microscopy; TEM, transmission electron microscopy.

connect with hydrophilic groups of the micelle shells through hydrogen bonding, and finally, SiO₂ deposited around the micelles. Figure 3B shows the surface morphologies of CS-SA/DOX and CS-SA/SiO₂/DOX nanoparticles.

SAXS analysis of CS-SA/SiO₂/DOX nanoparticles

SAXS analysis of CS-SA/SiO₂/DOX-8 and CS-SA/SiO₂/DOX-16 was carried out by using polycrystalline diffraction (RIGAKU D/MAX 2550/PC). As was seen in Figure 4, there were diffraction peaks in both CS-SA/SiO₂/DOX-8 and CS-SA/SiO₂/DOX-16 SAXS images. From the diffraction peaks in SAXS images, it can be concluded that CS-SA/SiO₂/DOX nanoparticles had periodic surface structures, indicating that mesopores appeared after SiO₂ deposition onto micelles.

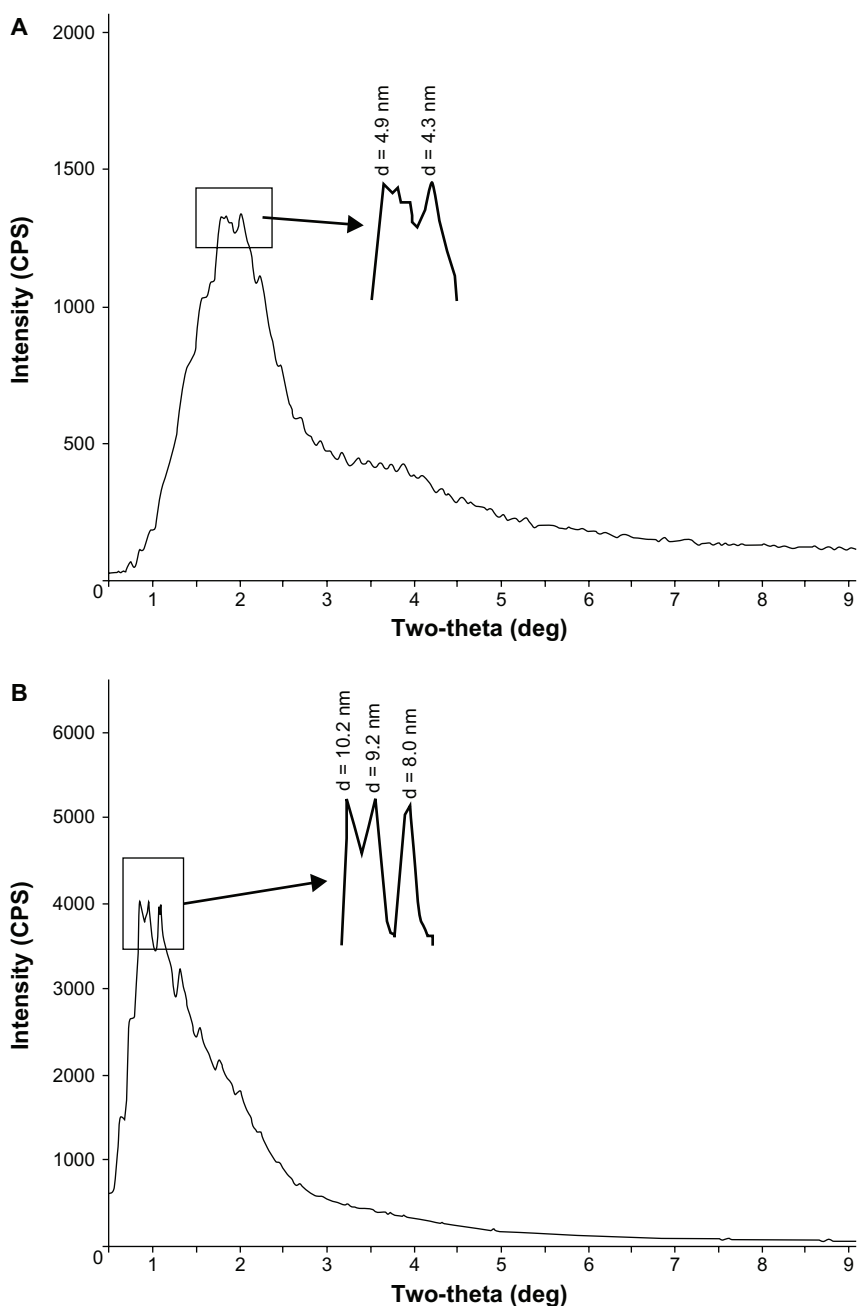


Figure 4 The SAXS images of CS-SA/SiO₂/DOX-8 (**A**) and CS-SA/SiO₂/DOX-16 (**B**).

Abbreviations: CS, chitosan; DOX, doxorubicin; SA, stearic acid; SAXS, small-angle X-ray scattering.

The pore size could be calculated from the angles of related diffraction peaks. There were two main diffraction peaks for CS-SA/SiO₂/DOX-8, with related pore sizes of 4.3 nm and 4.9 nm, respectively. For CS-SA/SiO₂/DOX-16, there were three salient diffraction peaks, whose related pore sizes were 8.0 nm, 9.2 nm, and 10.2 nm, respectively.

In vitro release assay

As shown in Figure 5, the cumulative DOX release rate of CS-SA/DOX, CS-SA/SiO₂/DOX-4, CS-SA/SiO₂/DOX-8,

and CS-SA/SiO₂/DOX-16 nanoparticles within 48 h reached 56.9%, 84.7%, 91.4%, and 89.4%, respectively. It can be concluded that CS-SA/SiO₂/DOX nanoparticles presented a faster drug-release behavior than CS-SA/DOX micelles. This may be attributed to the different structures of CS-SA/DOX micelles and CS-SA/SiO₂/DOX nanoparticles. When SiO₂ deposited onto the CS-SA micelle, the mesopore structure of CS-SA/SiO₂/DOX nanoparticles made the specific surface area of CS-SA/SiO₂/DOX much larger than that of CS-SA/DOX micelles, and therefore the drug could release from

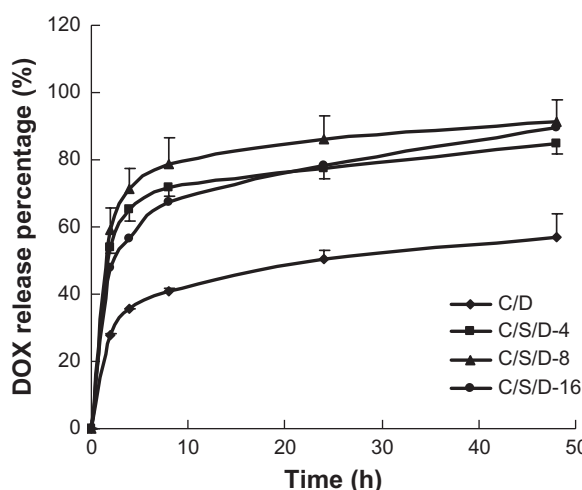


Figure 5 In vitro release profiles of CS-SA/DOX and CS-SA/SiO₂/DOX-4, -8, and -16.
Abbreviations: CS, chitosan; DOX, doxorubicin; SA, stearic acid.

the mesopores in a relatively short time in contrast with CS-SA/DOX micelles. However, no significant difference in drug-release behavior was observed from CS-SA/SiO₂/DOX with different SiO₂-deposited ratios, indicating that it was the existence of the mesopore rather than the size of the mesopore that influenced drug-release behavior.

Cellular uptake

Cellular uptake behaviors of CS-SA/DOX micelles and CS-SA/SiO₂/DOX nanoparticles were conducted using A549 cells. Figure 6 shows fluorescence microscope

images of A549 cells after incubation with CS-SA/DOX micelles or CS-SA/SiO₂/DOX-4 (8, 16) nanoparticles for different times (1, 4, 12, and 24 hours). It can be clearly seen in Figure 6 that, compared with CS-SA/DOX micelles, CS-SA/SiO₂/DOX nanoparticles could be taken up by A549 cells more rapidly, and that CS-SA/SiO₂/DOX nanoparticles can enter cells more easily with increasing SiO₂-deposited ratios.

Cytotoxicity assay

The IC₅₀ values of CS-SA/DOX micelles, CS-SA/SiO₂/DOX-4, CS-SA/SiO₂/DOX-8, CS-SA/SiO₂/DOX-16 nanoparticles against A549 cells measured using the MTT assay were 1.69, 0.93, 0.32, and 0.12 µg/mL, respectively (Figure 7). It could be concluded that CS-SA/SiO₂/DOX nanoparticles present a higher cytotoxicity than CS-SA/DOX micelles. Furthermore, an increase in cytotoxicity was observed for CS-SA/SiO₂/DOX nanoparticles with higher SiO₂-deposited ratios. The difference in cytotoxicity between CS-SA/SiO₂/DOX-16 nanoparticles and CS-SA/DOX micelles may be due to the different drug release rate and drug-loading capacity. As discussed in the “In vitro release assay” section, CS-SA/SiO₂/DOX nanoparticles showed faster drug release behaviors than CS-SA/DOX micelles in vitro. Additionally, it was described in the “Cellular uptake” section that CS-SA/SiO₂/DOX nanoparticles could enter into cells

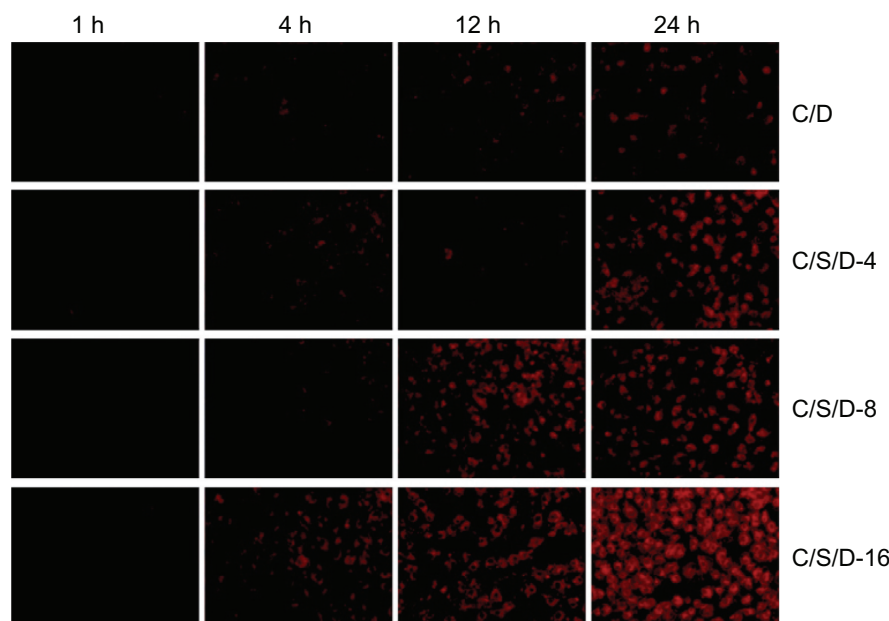


Figure 6 Fluorescent microscopic images of co-cultured A549 cells with CS-SA/DOX, CS-SA/SiO₂/DOX-4, CS-SA/SiO₂/DOX-8, and CS-SA/SiO₂/DOX-16 at different time points (1, 4, 12, and 24 hours).

Abbreviations: CS, chitosan; DOX, doxorubicin; SA, stearic acid.

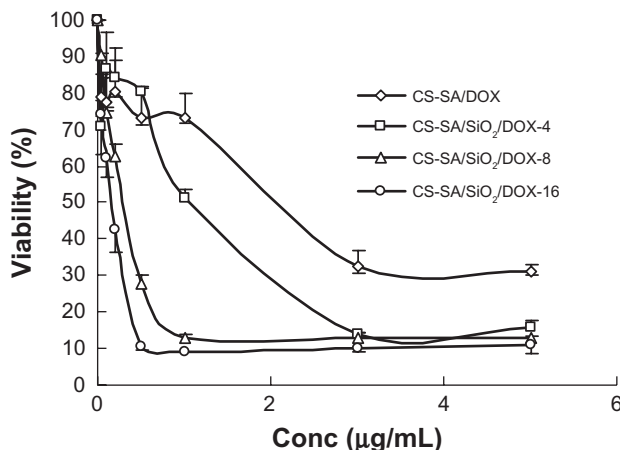


Figure 7 Plots of A549 cellular viability against CS-SA/DOX, CS-SA/SiO₂/DOX-4, CS-SA/SiO₂/DOX-8, and CS-SA/SiO₂/DOX-16 over 24 hours.

Abbreviations: CS, chitosan; DOX, doxorubicin; SA, stearic acid.

more easily than CS-SA/DOX micelles. A fast drug-release rate and enhanced cellular uptake capacity resulted in a large amount of DOX internalized into cells in a relatively short time when CS-SA/SiO₂/DOX nanoparticles were incubated with A549 cells. For CS-SA/SiO₂/DOX nanoparticles with different SiO₂-deposited ratios (CS-SA/SiO₂/DOX-4, CS-SA/SiO₂/DOX-8, and CS-SA/SiO₂/DOX-16), there was no significant difference in drug-release behaviors. However, cellular internalization became easier with an increased SiO₂-deposited ratio, and a higher ratio of SiO₂-deposited resulted in higher cytotoxicity caused by CS-SA/SiO₂/DOX nanoparticles.

Conclusion

In this study, stearic acid-grafted chitosan (CS-SA) was synthesized and could easily self-assemble into micelles. Thus, SiO₂-deposited DOX-loaded CS-SA (CS-SA/SiO₂/DOX) nanoparticles were successfully prepared under mild conditions using TEOS as a silica precursor. Crosslinking by silica resulted in CS-SA/SiO₂/DOX nanoparticles with a mesoporous structure; sizes of mesopores varied with different SiO₂-deposited ratios. Compared with normal DOX-loaded CS-SA (CS-SA/DOX) micelles, CS-SA/SiO₂/DOX had a more rapid drug release rate in vitro and could enter into the cells more easily. Higher cytotoxicity has been observed with increasing of SiO₂-deposited ratios of CS-SA/SiO₂/DOX nanoparticles.

Acknowledgments

We appreciate the financial support from the National Basic Research Program of China (973 Program) under Contract 2009CB930300, Key Project of Science and Technology of

Zhejiang Province (Grant No 2009C13037), and Zhejiang Provincial Program for the Cultivation of High-level Innovative Health Talents.

Disclosure

The authors report no conflicts of interest in this work.

References

- Orive G, Hernández RM, Gascón AR, Pedraz JL. Micro and nano drug delivery systems in cancer therapy. *Cancer Therapy*. 2005;3:131–138.
- Webber SE. Polymer micelles: an example of self-assembling polymers. *J Phys Chem B*. 1998;102(15):2618–2626.
- Maeda H, Wu J, Sawa T, Matsumura Y, Hori K. Tumor vascular permeability and the EPR effect in macromolecular therapeutics: a review. *J Control Release*. 2000;65:271–284.
- Matsumura Y, Kataoka K. Preclinical and clinical studies of anticancer agent – incorporating polymer micelles. *Cancer Sci*. 2009;100(4):572–579.
- Husseini GA, Pitt WG. Micelles and nanoparticles for ultrasonic drug and gene delivery. *Adv Drug Deliv Rev*. 2008;60(10):1137–1152.
- Hu FQ, Meng P, Dai YQ, et al. PEGylated chitosan-based polymer micelle as an intracellular delivery carrier for anti-tumor targeting therapy. *Eur J Pharm Biopharm*. 2008;70(3):749–757.
- Huang MH, Chou AH, Lien SP, et al. Formulation and immunological evaluation of novel vaccine delivery systems based on bioresorbable poly(ethylene glycol)-block-poly(lactideco-epsilon-caprolactone). *J Biomed Mater Res B Appl Biomater*. 2009;90(2):832–841.
- Bernkop-Schnürch A, Krajicek ME. Mucoadhesive polymers as platforms for peroral peptide delivery and absorption: synthesis and evaluation of different chitosan-EDTA conjugates. *J Control Release*. 1998;50(1–3):215–223.
- Kresge CT, Leonowicz ME, Roth WJ, Vartuli JC, Beck JS. Ordered mesoporous molecular sieves synthesized by a liquid-crystal template mechanism. *Nature*. 1992;359(6397):710–712.
- Slowing II, Vivero-Escoto JL, Wu CW, Lin VSY. Mesoporous silica nanoparticles as controlled release drug delivery and gene transfection carriers. *Adv Drug Deliv Rev*. 2008;60(11):1278–1288.
- Slowing II, Trewyn BG, Giri S, Lin VSY. Mesoporous silica nanoparticles for intracellular delivery of membrane-impermeable proteins. *J Am Chem Soc*. 2007;129(28):8845–8849.
- Radu DR, Lai CY, Jeftinija K, Rowe EW, Jeftinija S, Lin VS. A polyamidoamine dendrimer-capped mesoporous silica nanosphere-based gene transfection reagent. *J Am Chem Soc*. 2004;126(41):13216–13217.
- Simovic S, Heard P, Hui H, et al. Dry hybrid lipid-silica microcapsules engineered from submicron lipid droplets and nanoparticles as a novel delivery system for poorly soluble drugs. *Mol Pharm*. 2009;6(3):861–872.
- Tan A, Simovic S, Davey AK, Rades T, Prestidge CA. Silica-lipid hybrid (SLH) microcapsules: a novel oral delivery system for poorly soluble drugs. *J Control Release*. 2009;134(1):62–70.
- Dwivedi N, Arunagirinathan MA, Sharma S, Bellare J. Silica-coated liposomes for insulin delivery. *J Nanomat*. 2010;652048.
- Mohanraj VJ, Barnes TJ, Prestidge CA. Silica nanoparticle coated liposomes: A new type of hybrid nanocapsule for proteins. *Int J Pharm*. 2010;392(1):285–293.
- Hu FQ, Ren GF, Yuan H, Du YZ, Zeng S, et al. Shell cross-linked stearic acid grafted chitosan oligosaccharide self-aggregated micelles for controlled release of paclitaxel. *Colloids Surf B Biointerfaces*. 2006;50(2):97–103.
- Wen J, Wilkes GL. Organic/inorganic hybrid network materials by the sol-gel approach. *Chem Mater*. 1996;8(8):1667–1681.

19. Li Y, Hu FQ, Yuan H. Preparation and release profiles of chitosan oligosaccharide grafted stearic acid nanoparticles in vitro. *Chinese Pharm J.* 2005;40(14):1083.
20. Huang M, Ma Z, Khor E, Lim LY. Uptake of FITC-chitosan nanoparticles by A549 cells. *Pharm Res.* 2002;19(10):1488–1494.
21. Pieper JS, Hafmans T, Veerkamp JH, Kuppevelt TH. Development of tailor-made collagen-glycosaminoglycan matrices: EDC/NHS crosslinking, and ultrastructural aspects. *Biomaterials.* 2000;21(6): 581–593.
22. Hu FQ, Zhao MD, Yuan H, You J, Du YZ, Zeng S. A novel chitosan oligosaccharide-stearic acid micelles for gene delivery: properties and in vitro transfection studies. *Int J Pharm.* 2006;315(1–2):158–166.
23. Kohori F, Yokoyama M, Sakai K, Okano T. Process design for efficient and controlled drug incorporation into polymeric micelle carrier systems. *J Control Release.* 2002;78(1–3):155–163.

International Journal of Nanomedicine

Publish your work in this journal

The International Journal of Nanomedicine is an international, peer-reviewed journal focusing on the application of nanotechnology in diagnostics, therapeutics, and drug delivery systems throughout the biomedical field. This journal is indexed on PubMed Central, MedLine, CAS, SciSearch®, Current Contents®/Clinical Medicine,

Submit your manuscript here: <http://www.dovepress.com/international-journal-of-nanomedicine-journal>

Dovepress

Journal Citation Reports/Science Edition, EMBase, Scopus and the Elsevier Bibliographic databases. The manuscript management system is completely online and includes a very quick and fair peer-review system, which is all easy to use. Visit <http://www.dovepress.com/testimonials.php> to read real quotes from published authors.